Interferência e Difração

Refração

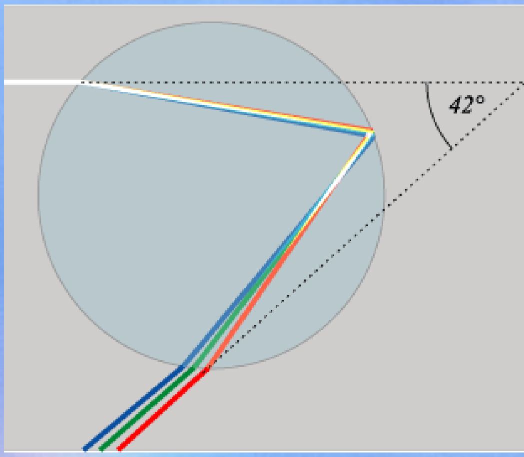

As cores vivas que vemos nas bolhas de sabão não são produzidas por refração, como as cores do arco-íris , mas por interferência

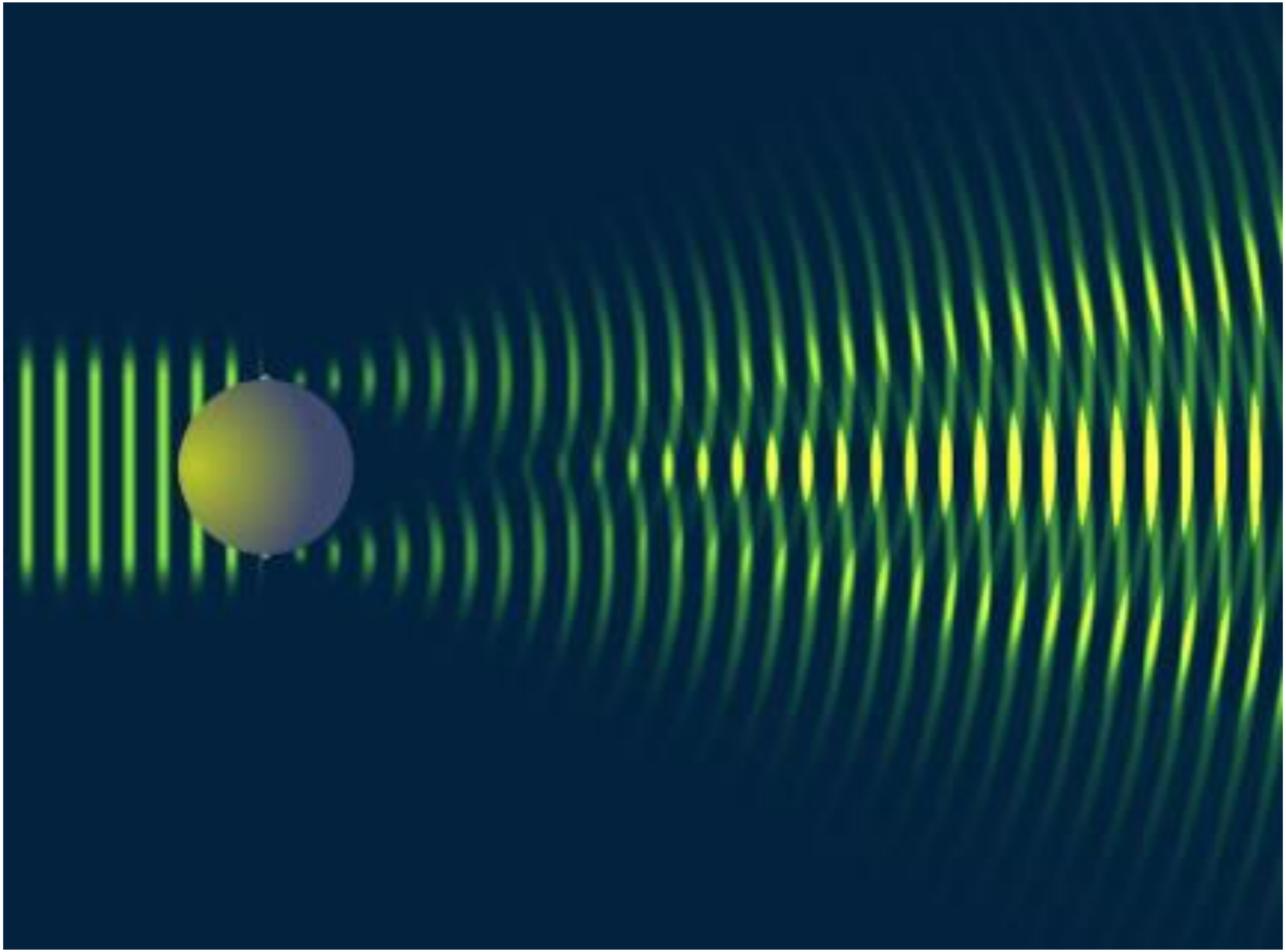

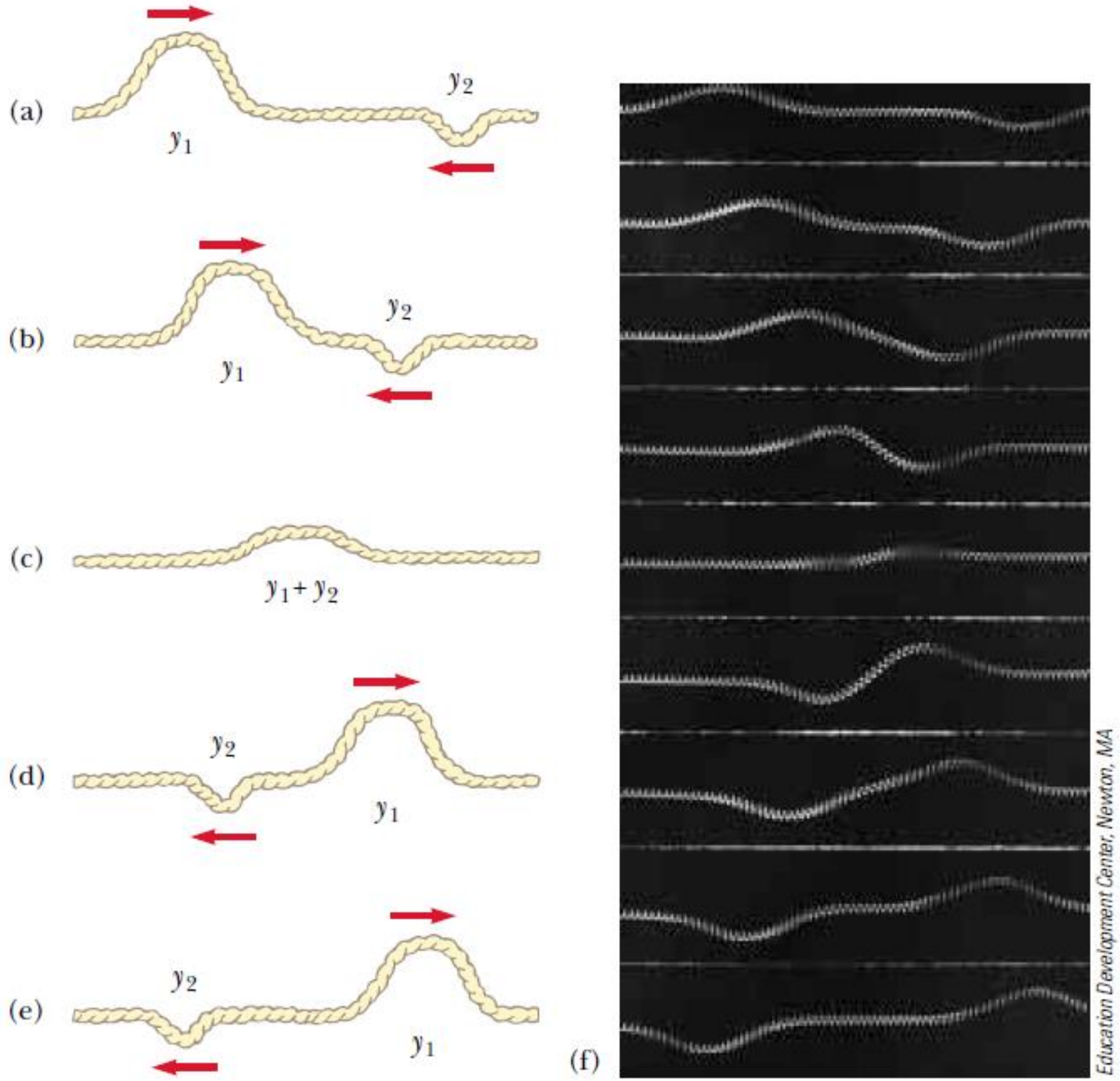
(a)
y_1
y_2
(b)
y_1
y_2
(c)
$y_1 + y_2$
(d)
y_2
y_1
(e)
y_2
y_1
(f)
Education Development Center, Newton, MA

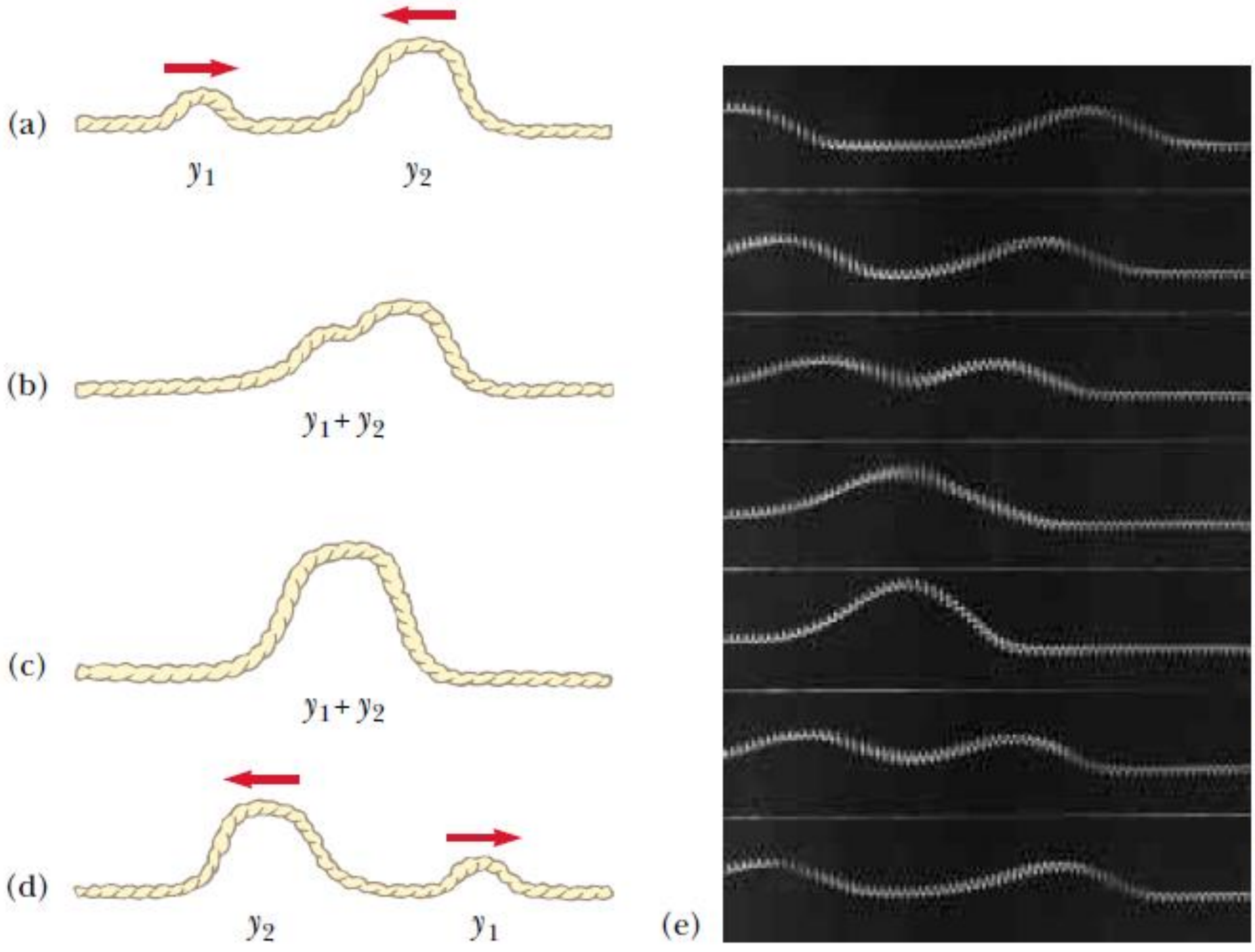

Education Development Center, Newton, MA

Luz – Onda Eletromagnética

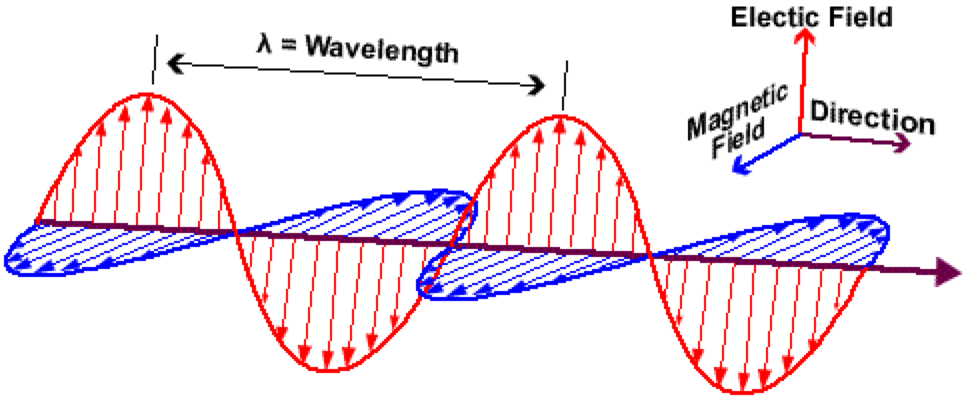

Fundamentalmente, toda interferência associada a ondas eletromagnéticas surge como resultado da combinação de campos elétrico e magnético que constituem a onda individual

Interferência de Ondas

Courtesy of Sabina Zigman/Benjamin Cardozo High School

At a beach in Tel Aviv, Israel, plane water waves pass through two openings in a breakwall. Notice the diffraction effect—the waves exit the openings with circular wave fronts, as in Figure 37.1b. Notice also how the beach has been shaped by the circular wave fronts.

O comportamento Ondulatório da Luz

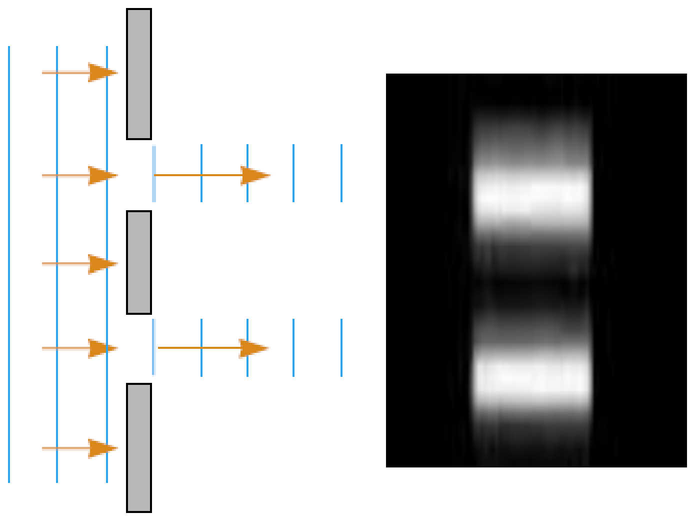

(a)

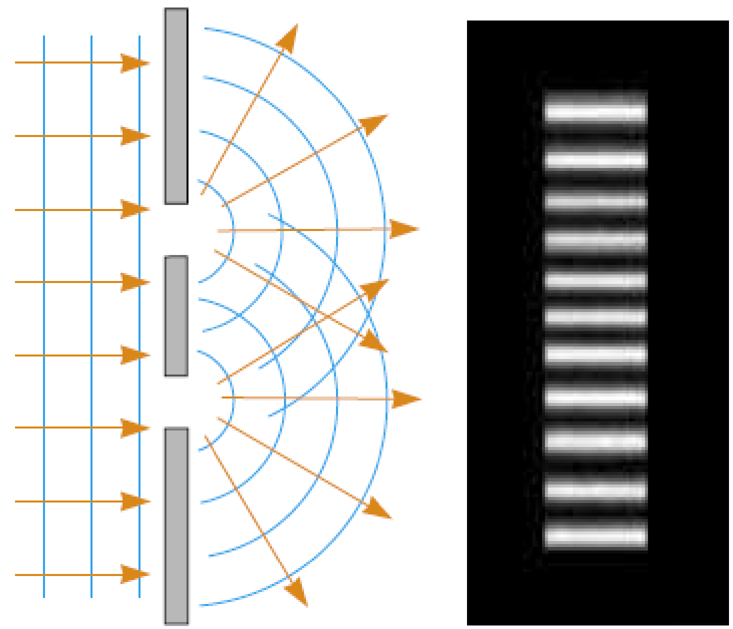

(b)

Experiência de Young da Dupla Fenda

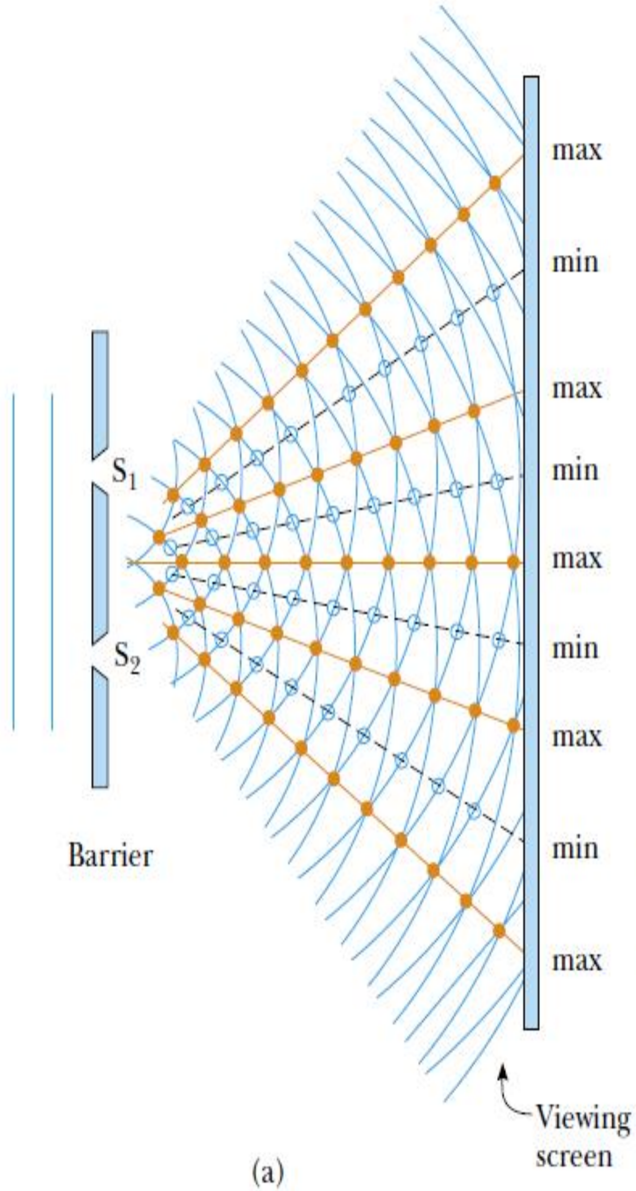

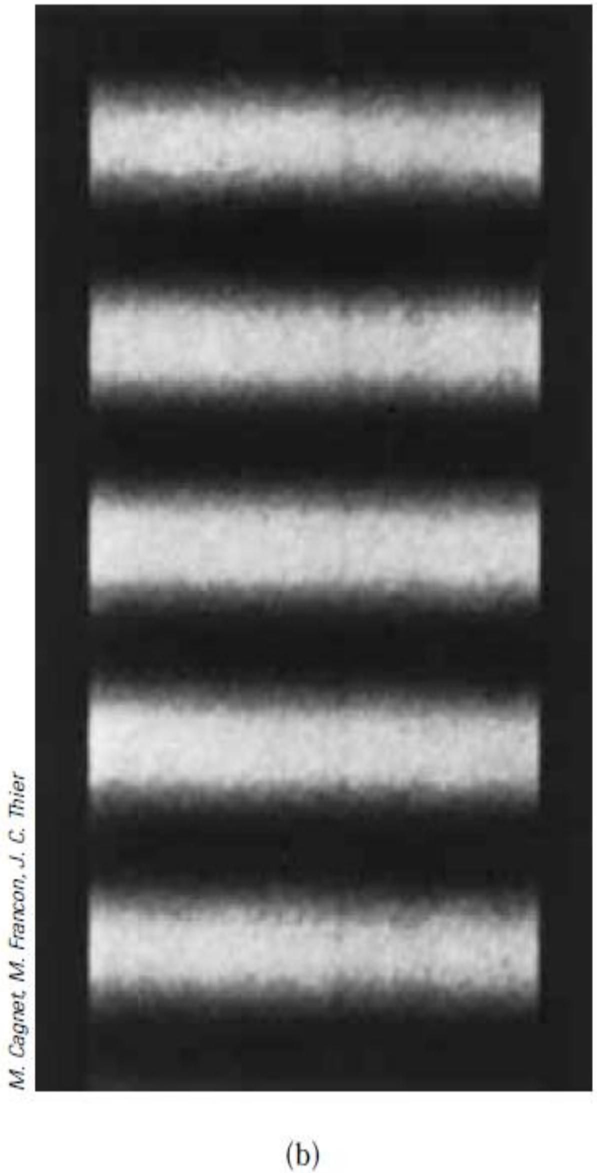

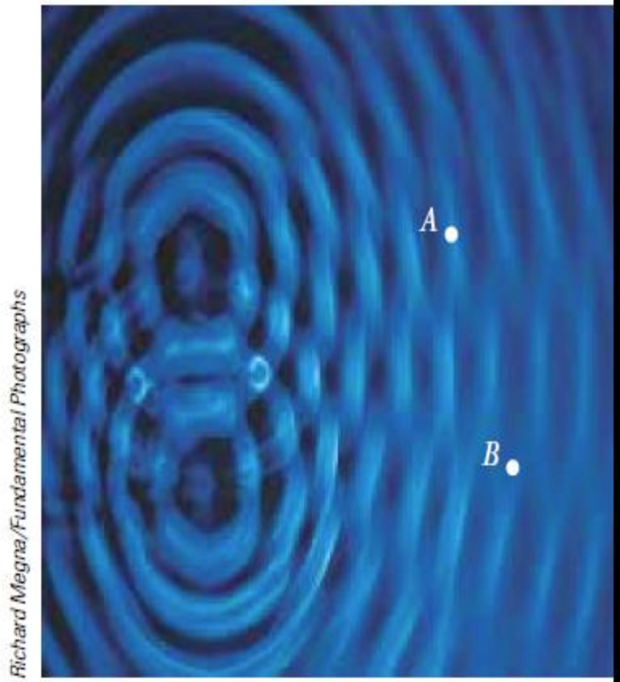

Figure 37.3 An interference pattern involving water waves is produced by two vibrating sources at the water's surface. The pattern is analogous to that observed in Young's double-slit experiment. Note the regions of constructive (*A*) and destructive (*B*) interference.

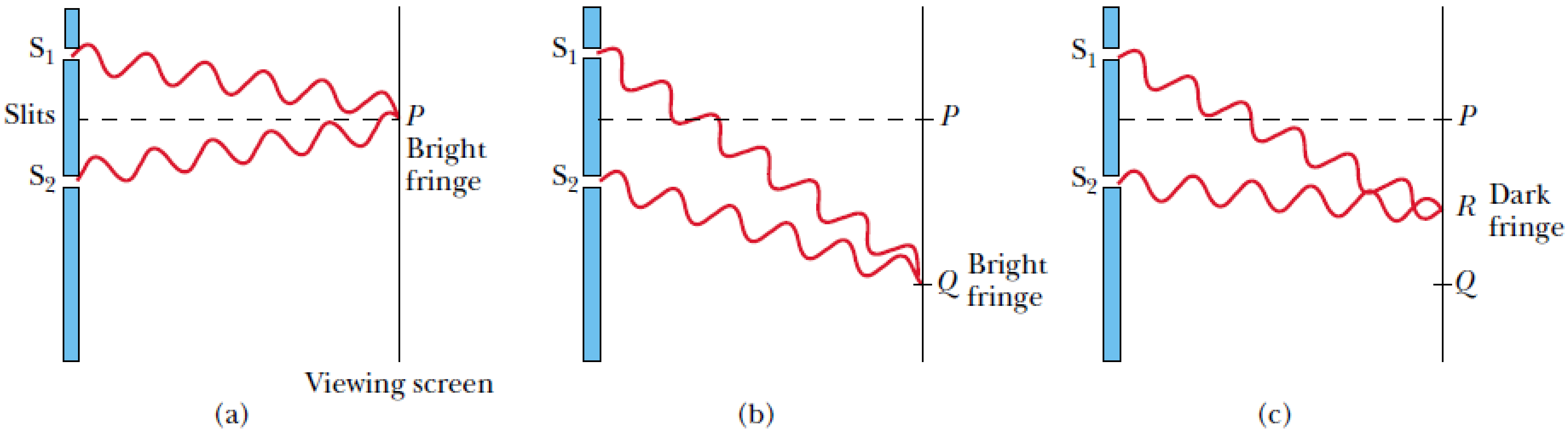

Figure 37.4 (a) Constructive interference occurs at point P when the waves combine. (b) Constructive interference also occurs at point Q. (c) Destructive interference occurs at R when the two waves combine because the upper wave falls half a wavelength behind the lower wave. (All figures not to scale.)

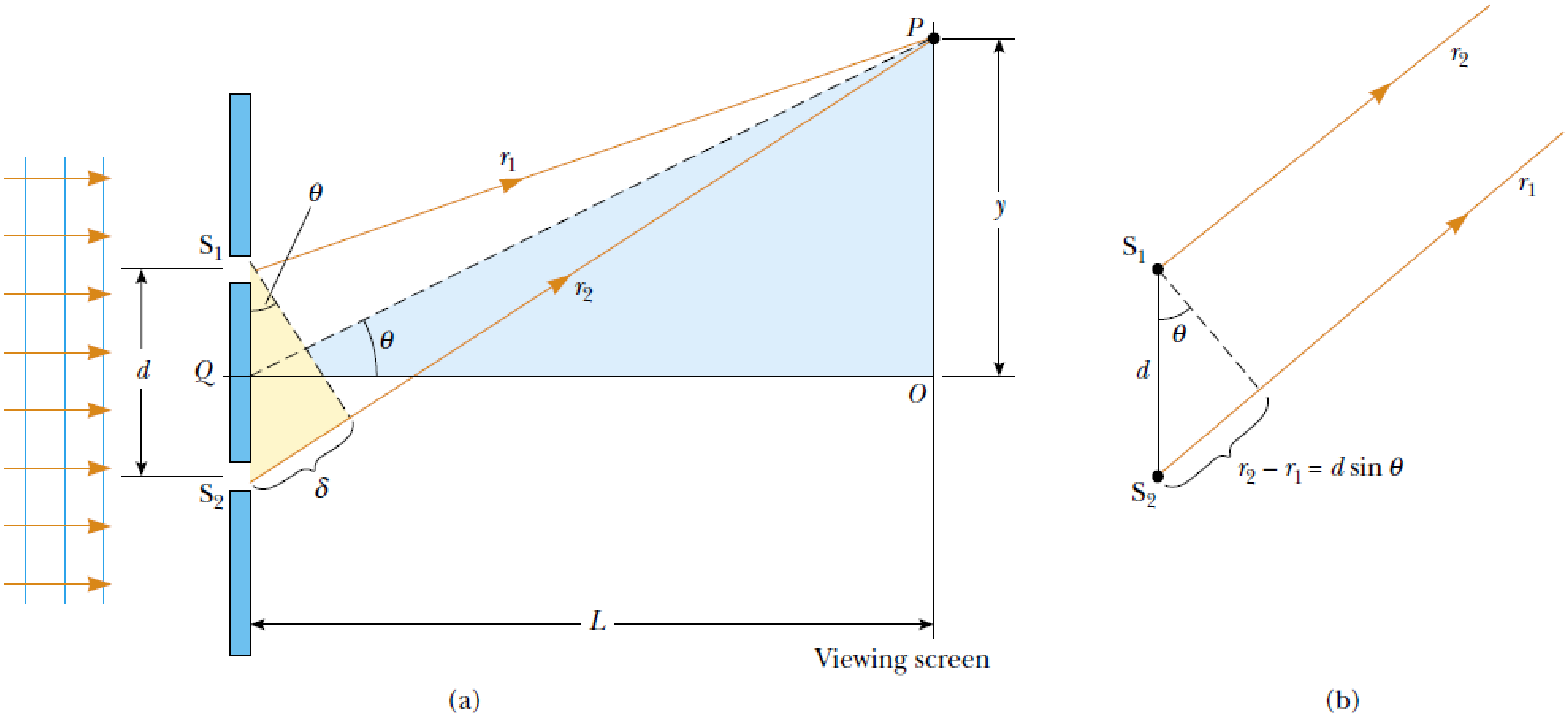

Figure 37.5 (a) Geometric construction for describing Young's double-slit experiment (not to scale). (b) When we assume that r_1 is parallel to r_2, the path difference between the two rays is $r_2 - r_1 = d \sin \theta$. For this approximation to be valid, it is essential that $L \gg d$.

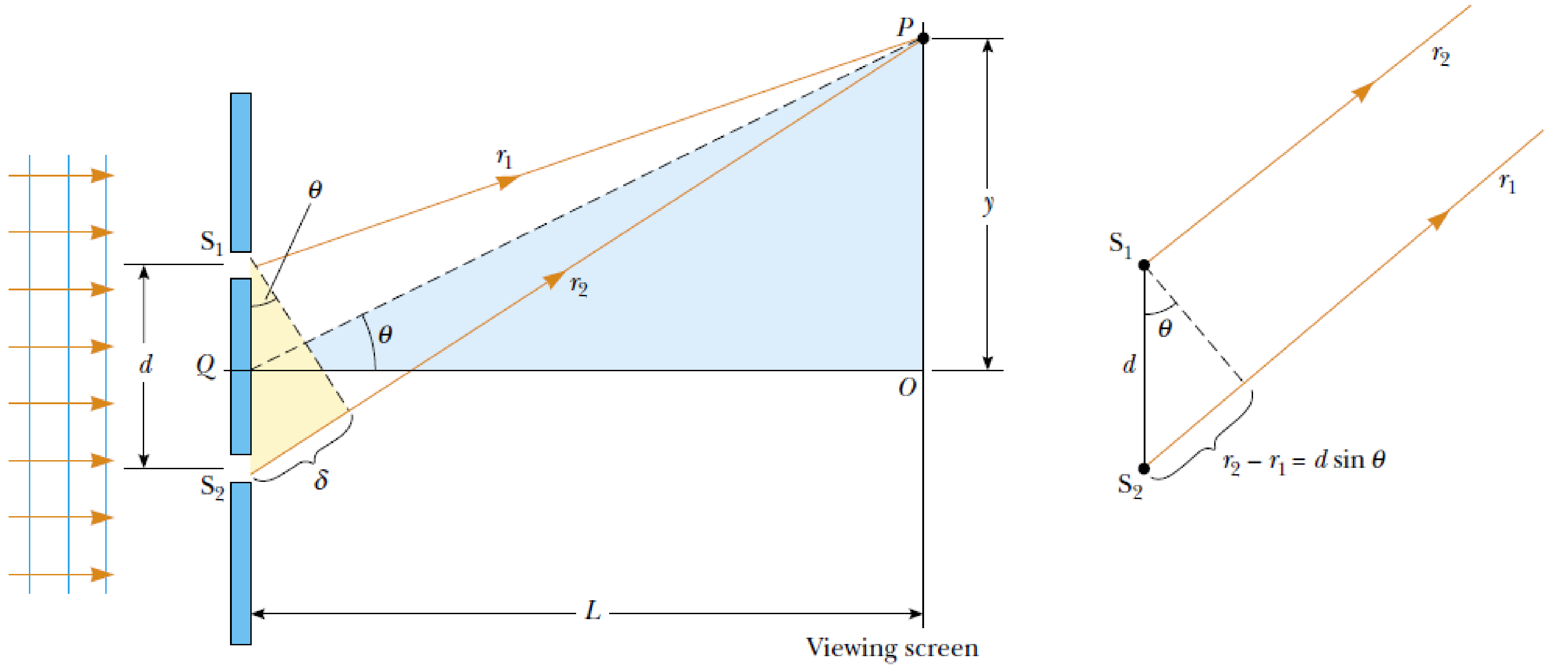

(a) (b)

L>>d

$$\delta = r_2 - r_1 = d.sen\theta$$

M = ordem da franja (central m=0)

Interferência Construtiva

$$\delta = r_2 - r_1 = d.sen\theta = m\lambda \ (m = 0, \pm 1, \pm 2, \dots)$$

Interferência destrutiva

$$\delta = r_2 - r_1 = d.sen\theta = \left(m + \frac{1}{2}\lambda\right)$$

$$(m = 0, \pm 1, \pm 2, \dots)$$

Expressões para as posições claras e escuras no anteparo

Além de L>>d, vamos assumir d>>λ, e θ também é pequeno, assim, nesse caso temos:

$$\sin\theta \approx \tan\theta$$

$$y = L\tan\theta \approx L\sin\theta$$

$$\boxed{y_{\text{bright}} = \frac{\lambda L}{d}\, m \qquad (m = 0, \pm 1, \pm 2, \ . \ . \ .)}$$

$$\boxed{y_{\text{dark}} = \frac{\lambda L}{d}\,(m + \tfrac{1}{2}) \qquad (m = 0, \pm 1, \pm 2, \ . \ . \ .)}$$

Difração em Fenda Única

Distribuição de Intensidade:

$$I \propto E_R^2$$

$$I = I_{\max}\left(\frac{sen\left(\frac{\beta}{2}\right)}{\frac{\beta}{2}}\right)^2 \quad , \quad \beta = \frac{2\pi}{\lambda} a sen\theta$$

$$\boxed{I = I_{\max}\frac{sen^2\left(\frac{\pi a sen\theta}{\lambda}\right)}{\left(\frac{\pi a sen\theta}{\lambda}\right)^2}}$$

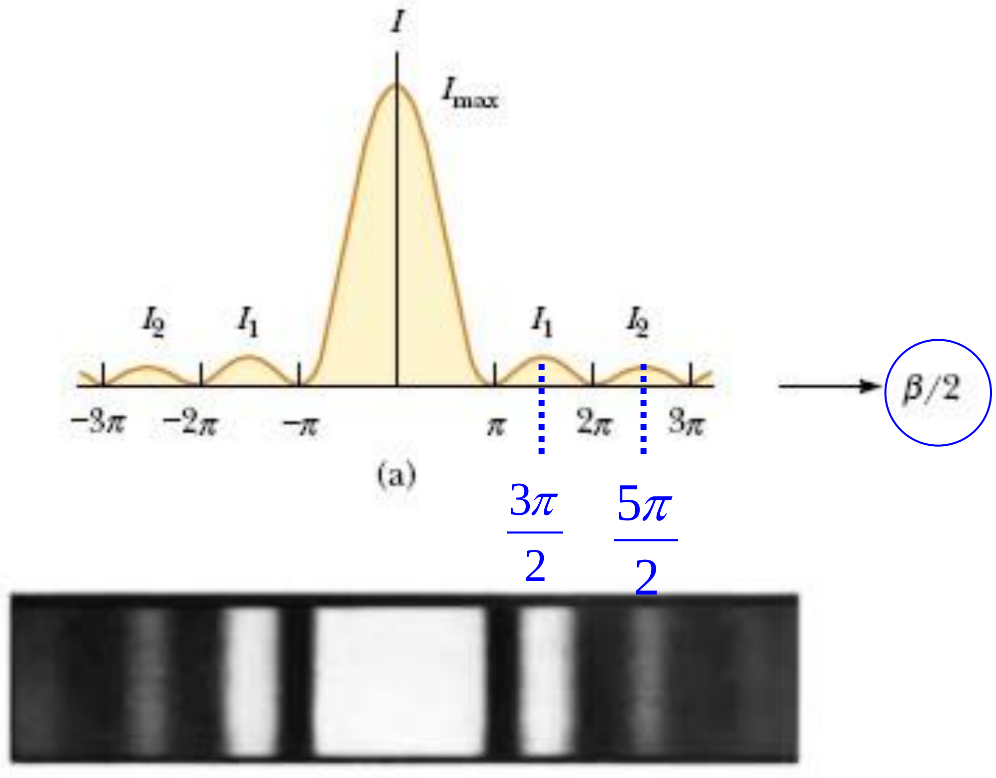

(a)

(b)

$$\frac{\beta}{2} = \frac{\pi a sen\theta}{\lambda} = m\pi, \quad m = \pm 1, \pm 2, \ldots$$

$$sen\theta = m\frac{\lambda}{a} \rightarrow \text{Mínimos}$$

Difração em Fenda Única

Difração Fraunhofer:

Luz espalhada

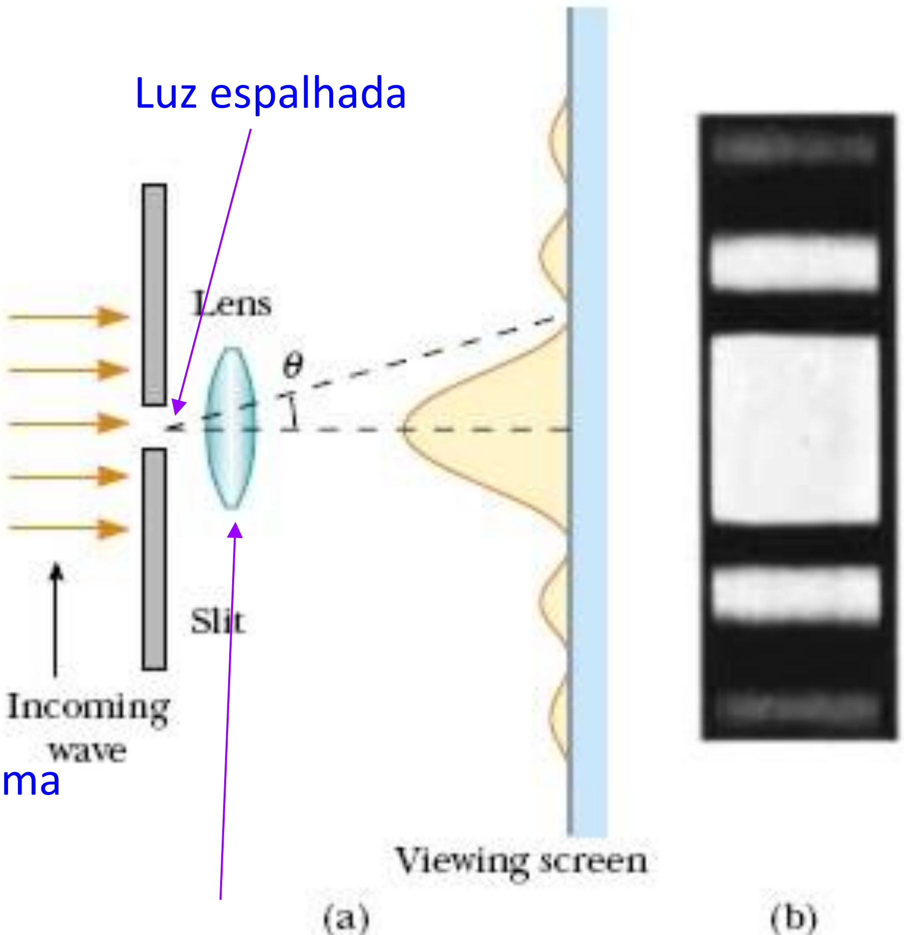

Raios paralelos provenientes de uma fonte de luz coerente (no plano focal obj. de uma lente convergente)

Focalizados no anteparo por outra lente convergente

Difração

Extremidade de um objeto:

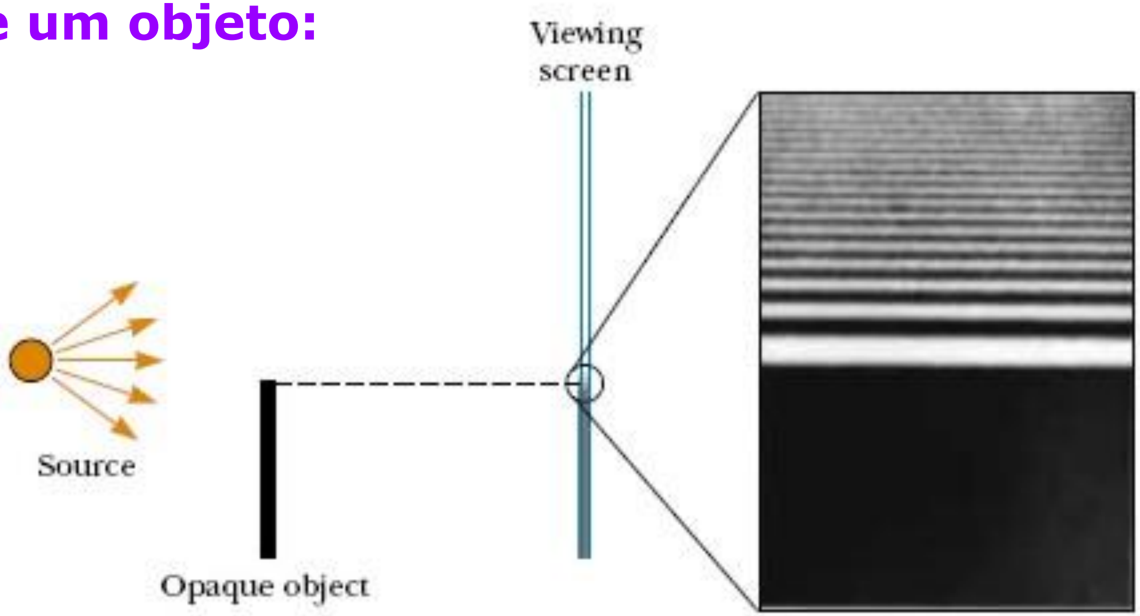

Objeto Circular:

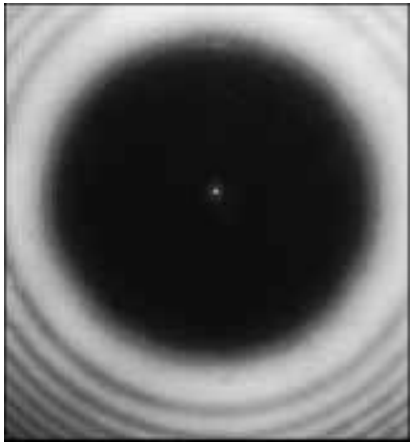

Dr. Jeremy Burgess/Science Photo Library

Peter Aprahamian/Science Photo Library/Photo Researchers, Inc.

(*Left*) Interference in soap bubbles. The colors are due to interference between light rays reflected from the front and back surfaces of the thin film of soap making up the bubble. The color depends on the thickness of the film, ranging from black where the film is thinnest to magenta where it is thickest. (*Right*) A thin film of oil floating on water displays interference, as shown by the pattern of colors when white light is incident on the film. Variations in film thickness produce the interesting color pattern. The razor blade gives you an idea of the size of the colored bands.

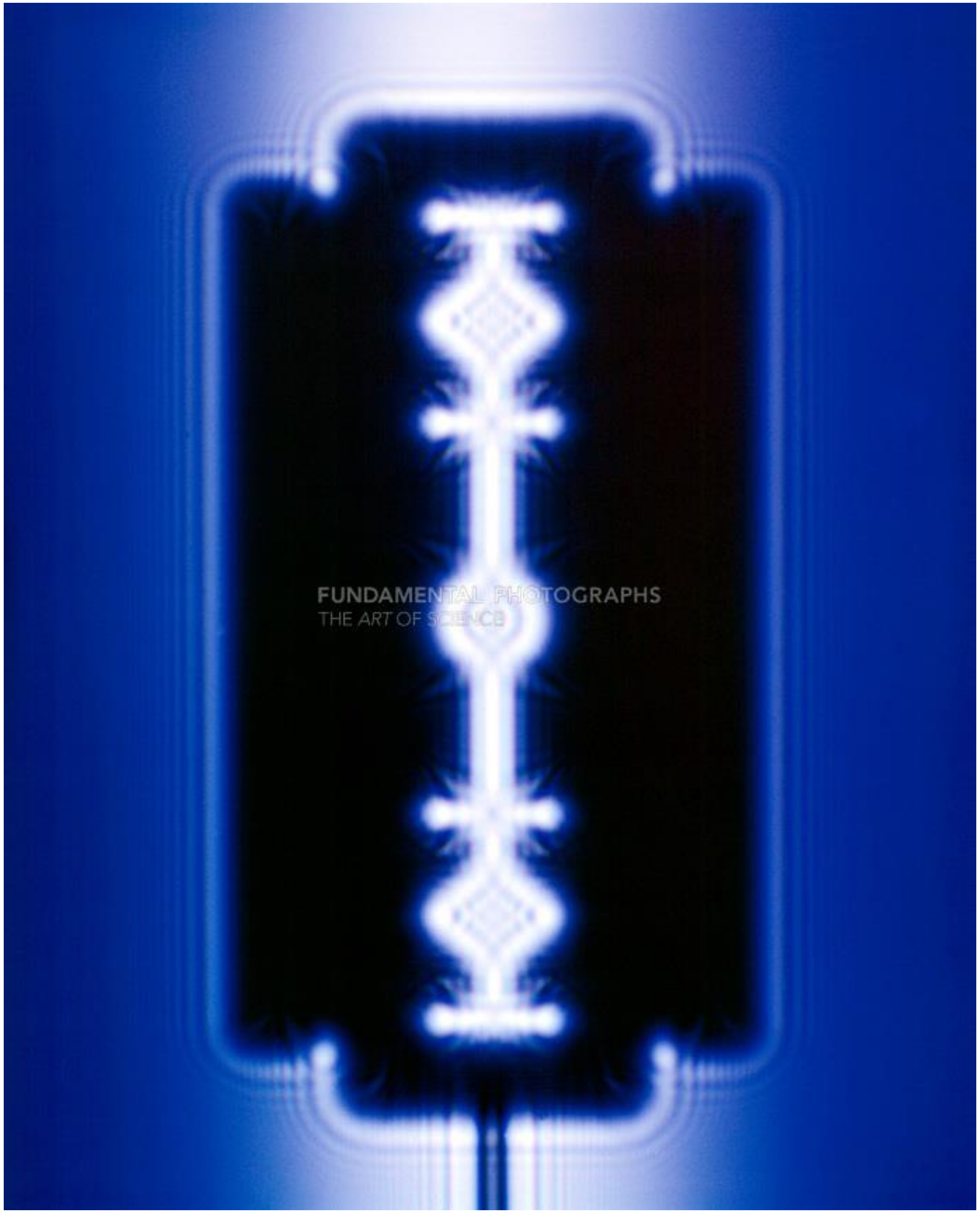

Interferência em filmes finos

- A wave traveling from a medium of index of refraction n_1 toward a medium of index of refraction n_2 undergoes a 180° phase change upon reflection when $n_2 > n_1$ and undergoes no phase change if $n_2 < n_1$.
- The wavelength of light λ_n in a medium whose index of refraction is n (see Section 35.5) is

$$\lambda_n = \frac{\lambda}{n}$$

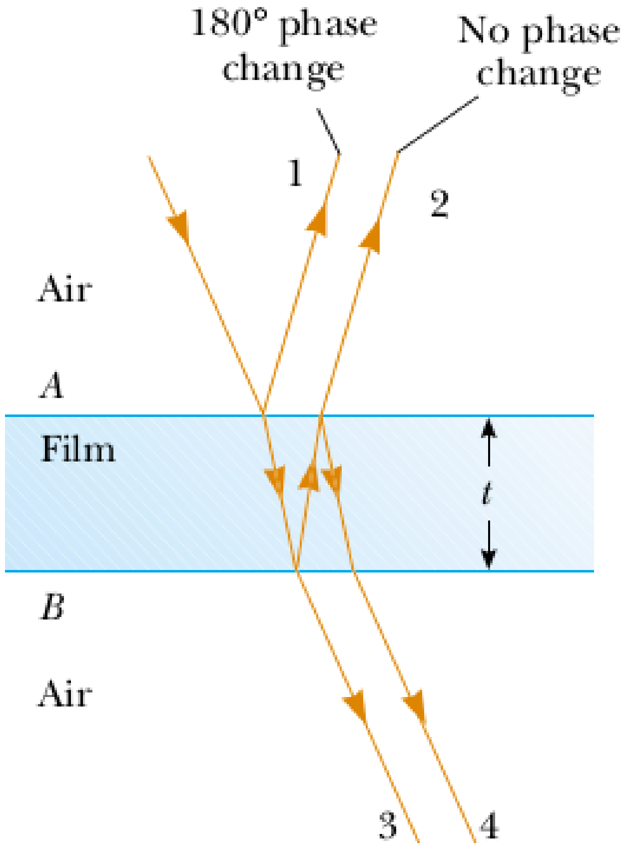

Interferência construtiva:

$$2t = (m + \tfrac{1}{2})\lambda_n \qquad (m = 0, 1, 2, \ . \ . \ .)$$

This condition takes into account two factors: (1) the difference in path length for the two rays (the term $m\lambda_n$) and (2) the 180° phase change upon reflection (the term $\lambda_n/2$). Because $\lambda_n = \lambda/n$, we can write Equation 37.15 as

$$2nt = (m + \tfrac{1}{2})\lambda \qquad (m = 0, 1, 2, \ . \ . \ .)$$

If the extra distance $2t$ traveled by ray 2 corresponds to a multiple of λ_n, then the two waves combine out of phase, and the result is destructive interference. The general equation for *destructive* interference in thin films is

$$2nt = m\lambda \qquad (m = 0, 1, 2, \ . \ . \ .)$$

Anéis de Newton

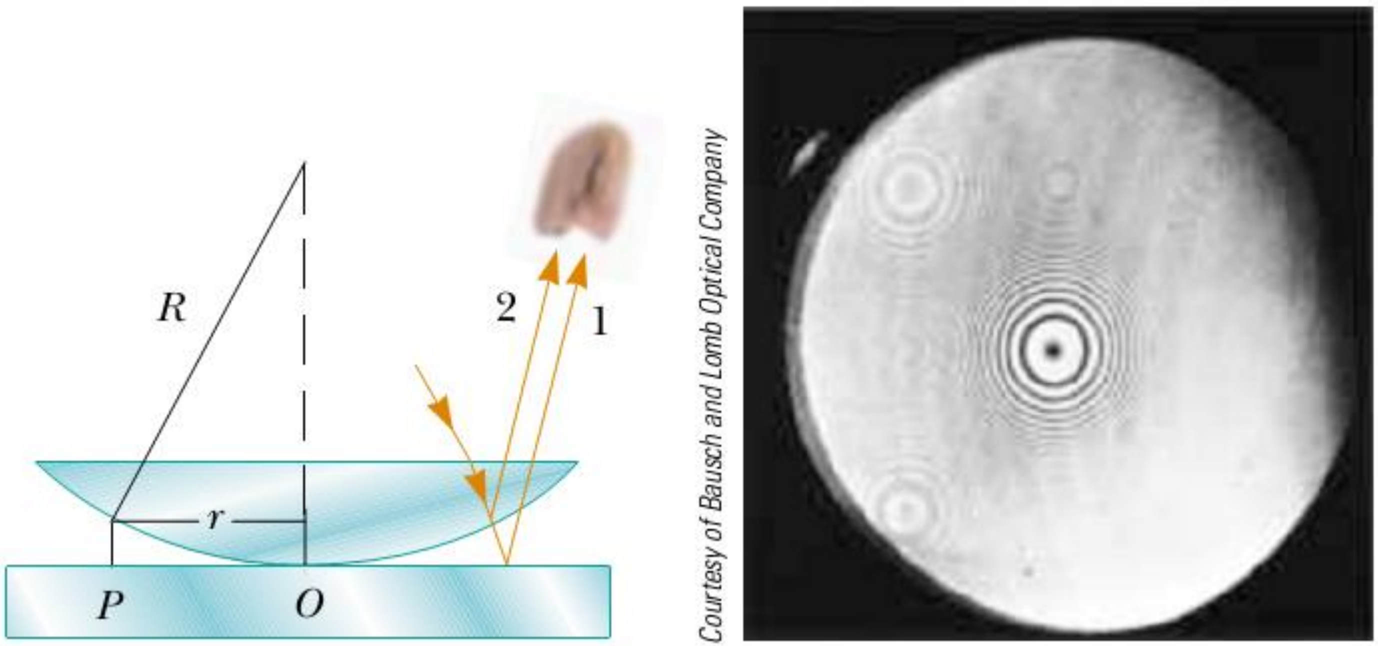

(a) (b)

Cunha

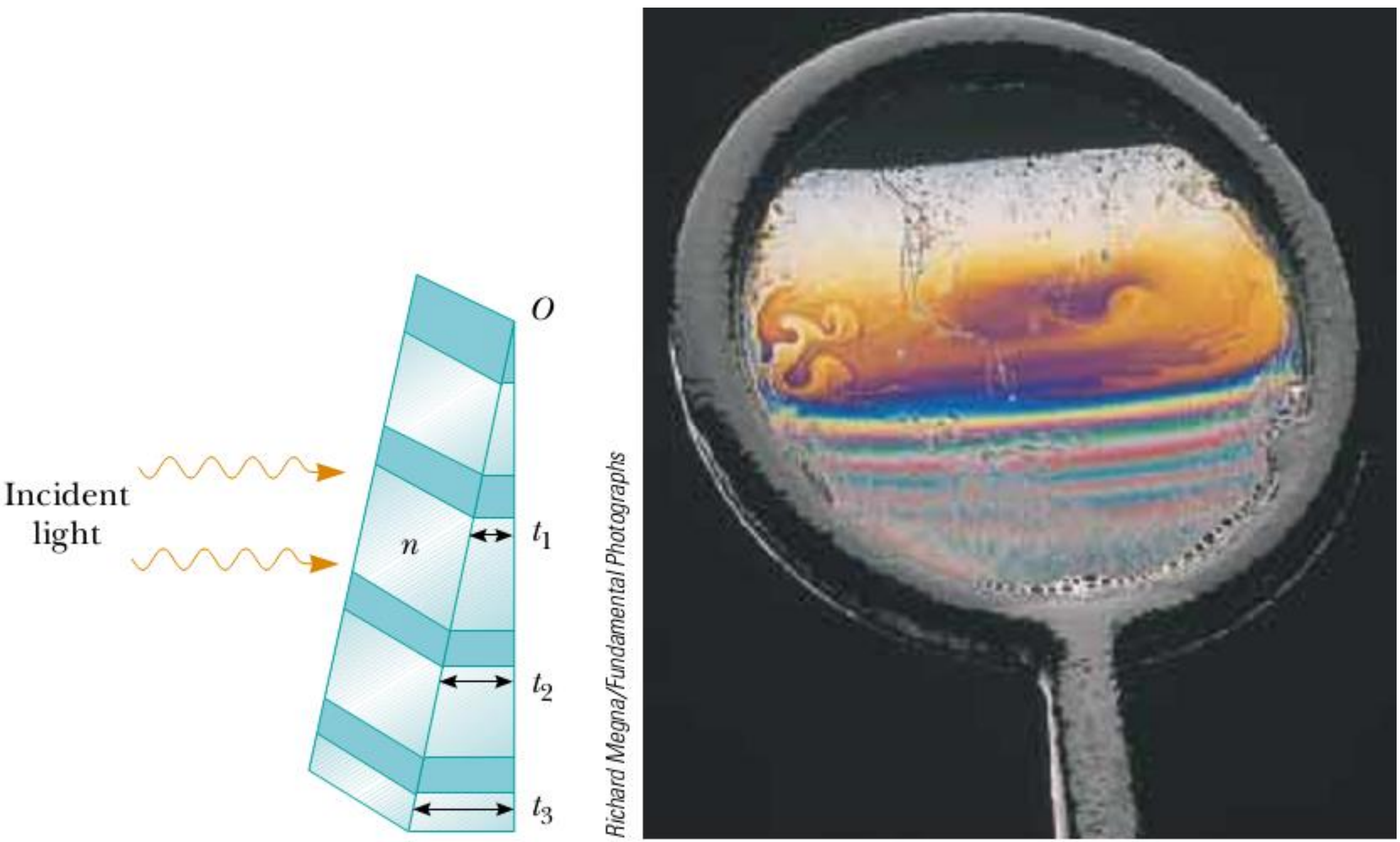
O
Incident light
n
t_1
t_2
t_3
Richard Megna/Fundamental Photographs

(a) (b)

Interferômetro de Michelson

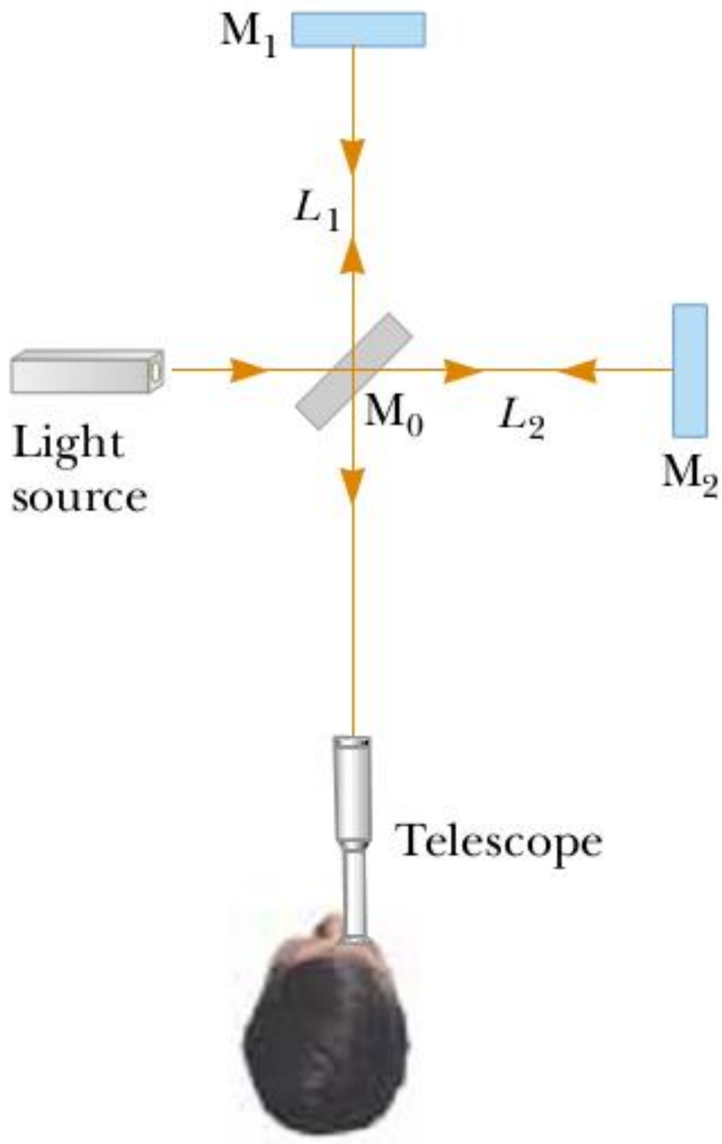

Lâmpada de Hidrogênio

4 comprimentos de onda na faixa
da luz visível.

Hélio

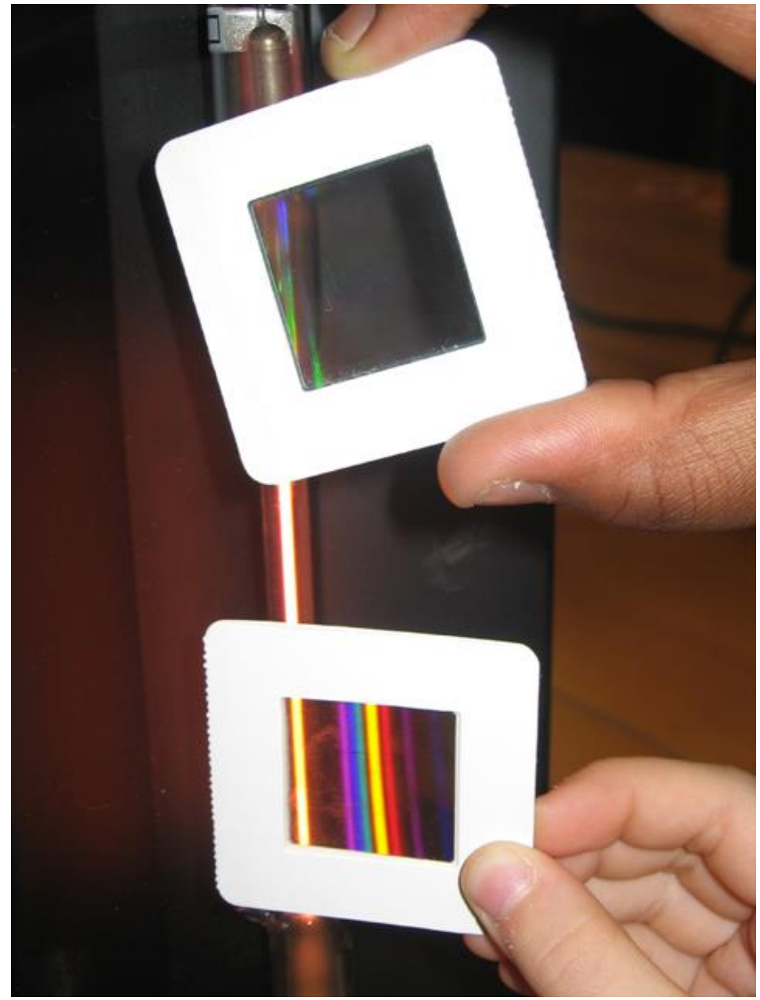

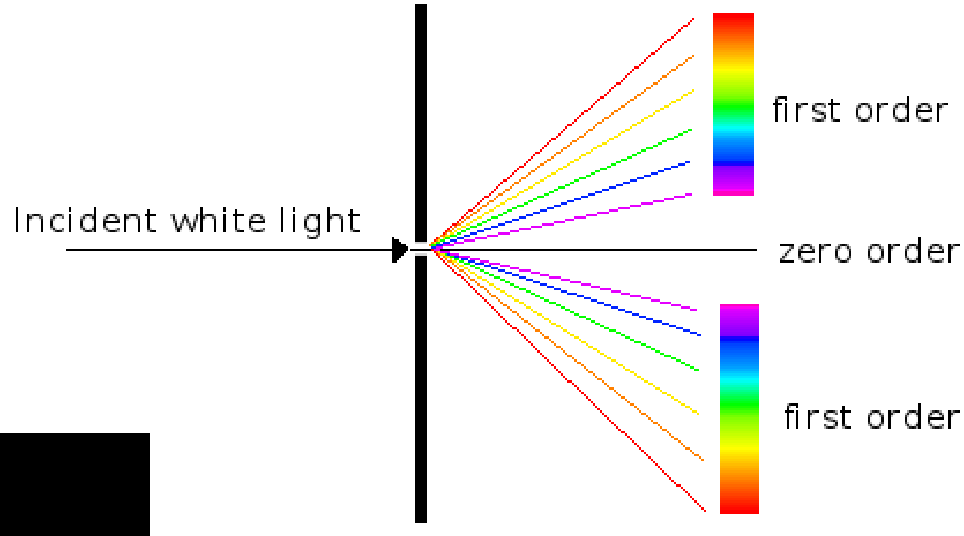
Incident white light
first order
zero order
first order

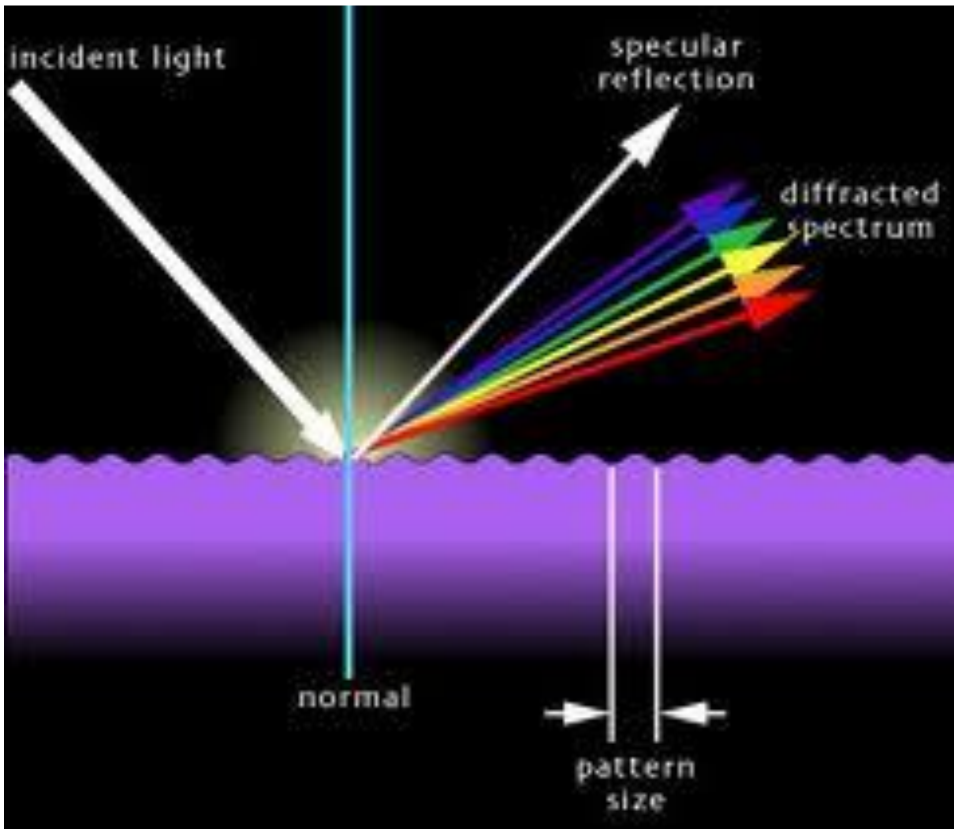
incident light
specular
reflection
diffracted
spectrum
normal
pattern
size

Redes de Difração

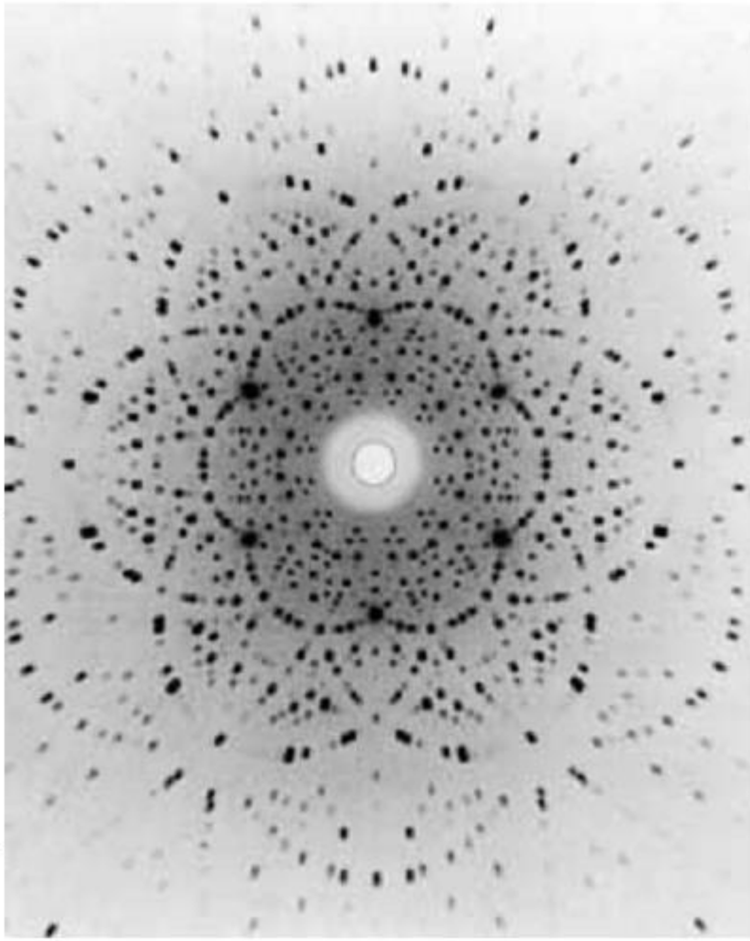

(a)

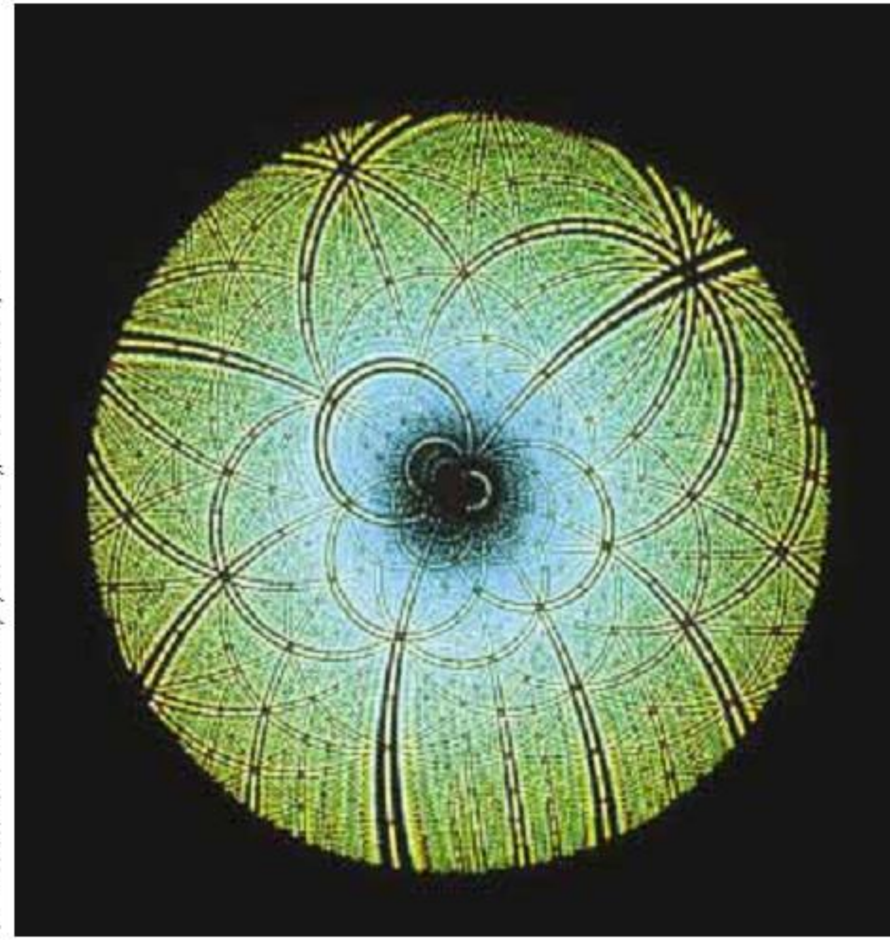

(b)

Figure 38.25 (a) A Laue pattern of a single crystal of the mineral beryl (beryllium aluminum silicate). Each dot represents a point of constructive interference. (b) A Laue pattern of the enzyme Rubisco, produced with a wide-band x-ray spectrum. This enzyme is present in plants and takes part in the process of photosynthesis. The Laue pattern is used to determine the crystal structure of Rubisco.

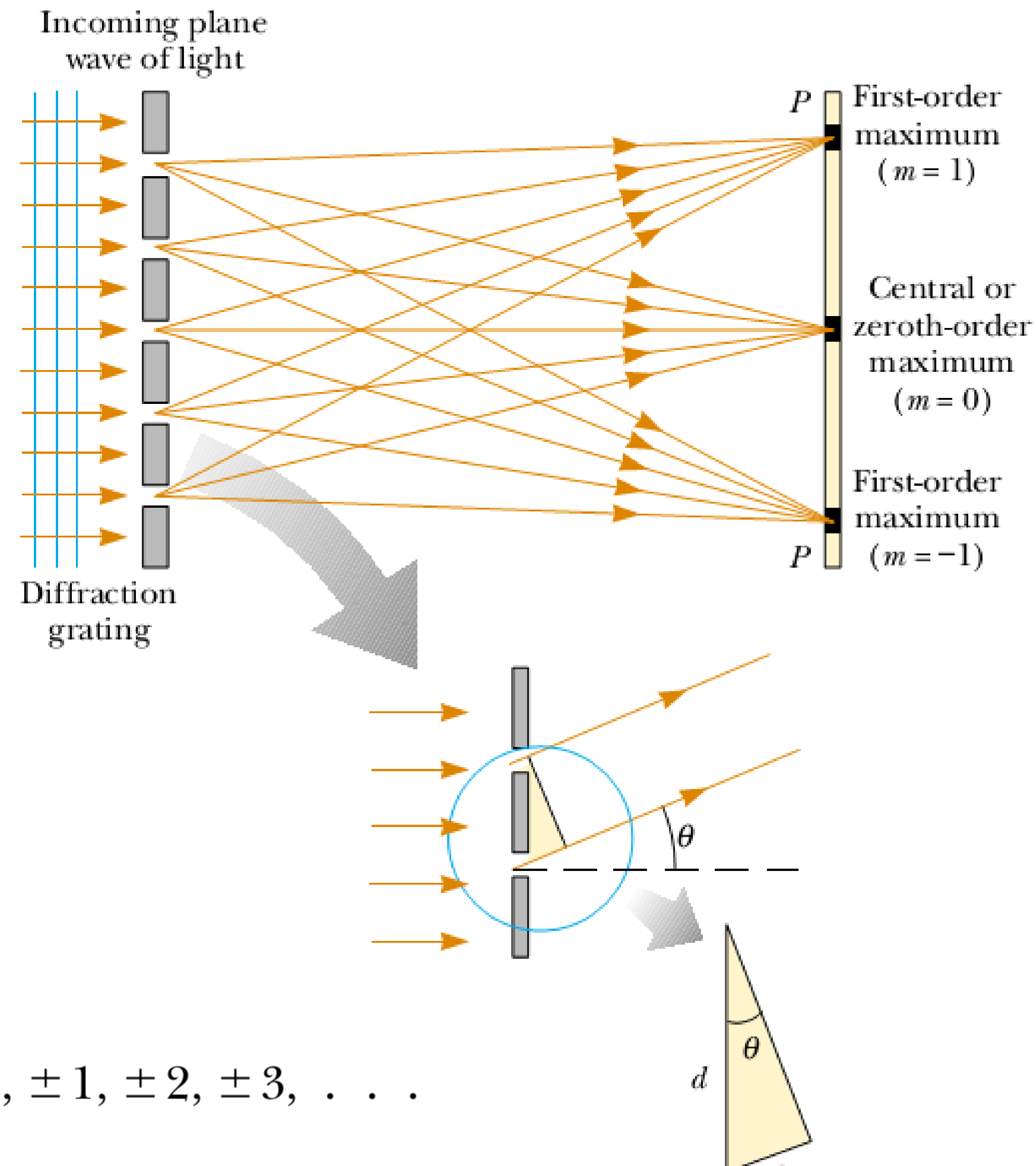

$$\boxed{d \sin \theta_{\text{bright}} = m\lambda}$$

$$m = 0, \pm 1, \pm 2, \pm 3, \ . \ . \ .$$

Figure 38.16 Side view of a diffraction grating. The slit separation is d, and the path difference between adjacent slits is $d \sin \theta$.

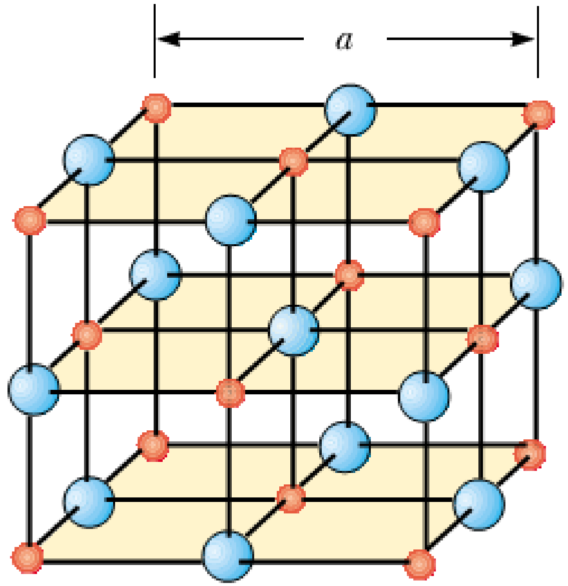

Figure 38.26 Crystalline structure of sodium chloride (NaCl). The blue spheres represent Cl^- ions, and the red spheres represent Na^+ ions. The length of the cube edge is $a = 0.562\,737$ nm.

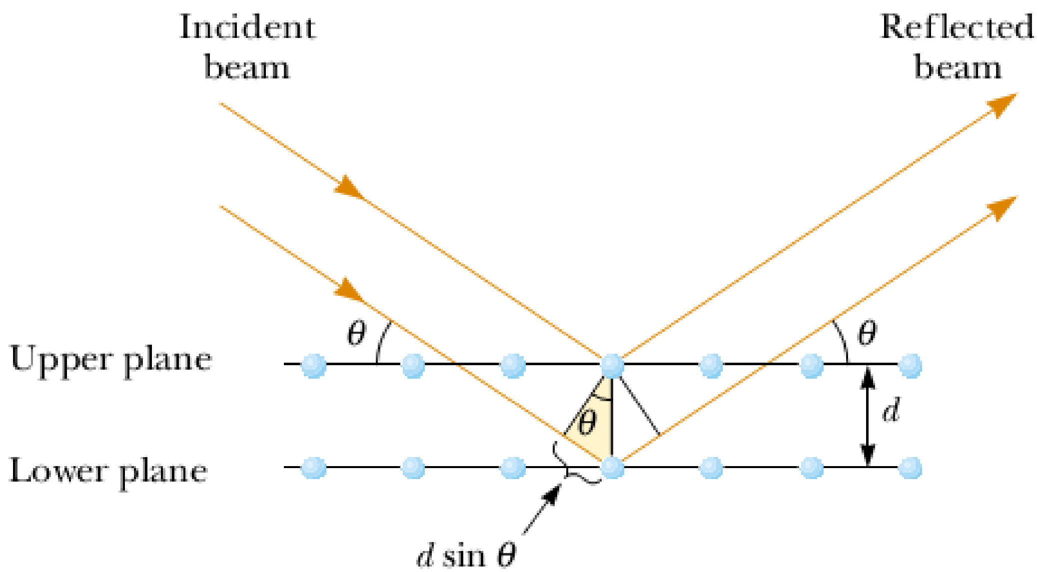

Figure 38.27 A two-dimensional description of the reflection of an x-ray beam from two parallel crystalline planes separated by a distance d. The beam reflected from the lower plane travels farther than the one reflected from the upper plane by a distance $2d \sin \theta$.

Lei de Bragg

$$2d \sin \theta = m\lambda \qquad m = 1, 2, 3, \ldots$$

$$\sin\,\theta_{\text{dark}} = m\,\frac{\lambda}{a} \qquad m = \pm 1, \pm 2, \pm 3, \ldots$$

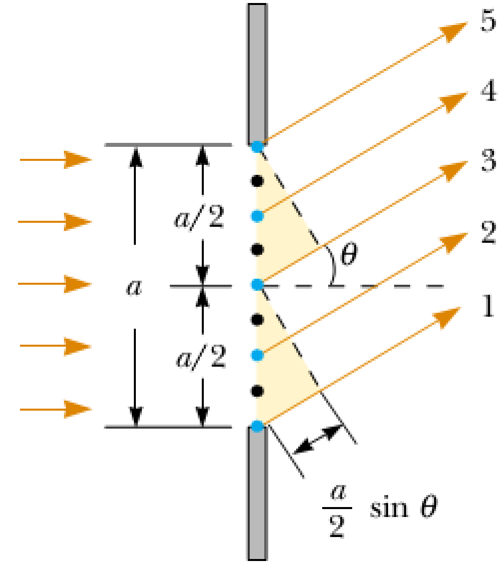

Figure 38.5 Paths of light rays that encounter a narrow slit of width a and diffract toward a screen in the direction described by angle θ. Each portion of the slit acts as a point source of light waves. The path difference between rays 1 and 3, rays 2 and 4, or rays 3 and 5 is $(a/2)\sin\theta$. (Drawing not to scale.)